Fibre device estimation techniques for SDM transmission

Chigo Okonkwo (*), Menno van den Hout, Sjoerd van der Heide and John van Weerdenburg

(*) High-Capacity Optical Transmission Laboratory, Electro-Optical Communications Group, Eindhoven University of Technology cokonkwo@tue.nl

Abstract *Space Division Multiplexing presents new impairments such as mode-dependent loss and. Differential mode dispersion, challenging to measure conventional processes. We discuss the feasibility of spatially diverse swept wavelength interferometry and digital holography techniques capable of measuring these characteristics, obtaining transfer matrices of devices.*

Introduction

As the bandwidth requirements in various parts of optical networks rapidly approach the limits of Single-mode fibre, research towards overcoming these limitations intensifies. Space Division Multiplexing has been long proposed as a technique exploiting data transmission over multiple modes and/or cores in a single fibre and has been shown as a promising candidate to overcome the SMF capacity limits [1]. It is expected that the first SDM deployments will be for applications requiring high-capacity short-reach interconnects, such as for inter-data centre connections, 5G front/back-hauling, high-capacity access links or amplifier pump sharing in trans-oceanic links [references].

While research towards SDM continues at a rapid pace, it has yet to be decided which fibre technology will be dominant in future optical transmission systems. Few-mode, multimode, and multi-core fibres (MCF) each have their own advantages and disadvantages [2,3]. The separation of spatial channels in multi-core fibres is easier compared to coupled core fibres, Few-mode fibre, Multimode fibre (MMF); however, MCF manufacturing is more challenging. FMF and MMF, on the other hand, potentially offer the highest capacity density but heavily rely on complex digital signal processing to recover the spatial channels. In addition to the fiber technology, components such as the single mode to SDM fiber interfaces, SDM amplifiers and Spatial wavelength selective switches (WSS) are being developed [2,3,4].

Additionally, SDM systems induce additional effects such as Mode dependent loss (MDL) and differential mode group delay. Currently, there are no off-the-shelf instruments for accurately characterising and testing SDM devices. Typically, devices are done by analysing equaliser taps through system-level measurements, but these are largely imprecise [3]. Therefore, a new generation of measurement techniques and instruments are required to measure and obtain transfer matrices of devices, fibres and components.

In this work, we discuss two main characterisation tools based on the spatially diverse Optical vector network analyser (OVNA) and the digital holography techniques. These systems both require specific digital signal processing algorithms to enable characteristics such as MDL, MDG and DMGD to be measured fast over a very large bandwidth.

Spatially Diverse Optical Vector Analyser

A comprehensive description of spatially diverse optical vector network analysers is given in [6]. The presented analysis is based on the group delay, derived from the frequency-dependent propagation constant of the optical field, but ignores any higher-order terms. This assumption is accurate when these effects are negligibly small, such as for slow sweeping rates and short device lengths. However, for optical vector network analysis of long fibers, higher-order transmission effects are captured within the propagation constant have to be taken into account.

The swept tunable laser (STL) source of the spatially-diverse OVNA, the coherent optical source must be capable of producing a linear-time frequency sweep resulting in the optical field depicted in figure 1 produces an optical field:

$$E_{STL}(t) = A_{STL}(t)e^{-j\omega(t)t}P_{STL}$$

Where A_{STL} is the complex amplitude andP_{STL} is the polarisation state at the output of the STL. The angular frequency $\omega(t) = 2\pi c/(\lambda_s + v(t)t)$ is the result of the sweep starting at λ_s with a sweep rate of $v(t)$. After propagation through an optical fiber of length z, the field is given by:

$$E\ (z,t) = A(z,t)e^{-jwt}e^{-j\beta\omega z}P\mathrm{z}$$

The simplest OVNA system consists of an optical source, an interferometric structure with fixed path lengths and the means to detect the signal as shown in Fig 1. A 1x M splitter and M delay-fiber lines are positioned between the polarisation multiplexer and the device under test.

978-1-6654-3868-1/21/$31.00 ©2021 IEEE

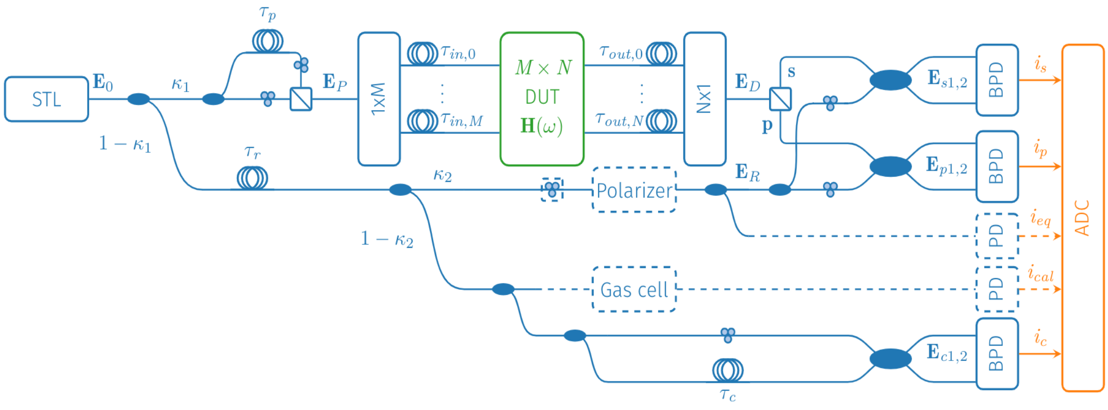

Figure 1: Spatially-diverse optical vector network analyser for 2M x 2N SDM components employing balanced photodetectors (BPDs)

At the output of each fiber, the optical field is a delayed copy with an arbitrary polarisation rotation. At the output of the device under test, the output port signals are guided through another set of fiber delays and an Mx1 coupler. Afterwards, balanced photo-detectors are required to receive the photo-currents. Analogue to digital converters is required to capture the samples for signal processing and extraction of the relevant metrics [7].

OVNA digital signal processing steps

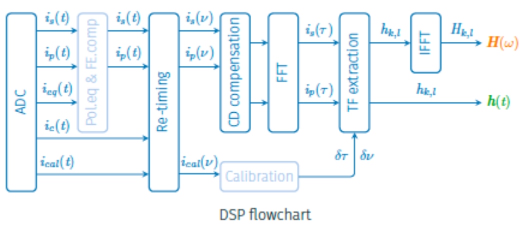

Figure 2: OVNA digital signal processing flow

Extracting the desired transfer function and impulse response matrices from the sampled photocurrents require several DSP steps as shown in Figure 2. The first DSP module compensates for the polarisation fading using both the data-signal and the polarisation tracking signal as input. By injecting a wide band signal with a flat spectrum, generated by shaping amplified spontaneous emission into the photodetectors, a frequency response estimation of the receiver is obtained. The non-flat response the ADC and power. fading introduced by polarisation rotations are compensated. The next module, converts the non-linear wavelength sweep to a linear frequency sweep by extracting new sample points from the received signal of the auxiliary clock interferometer. A bandpass filter is applied around the expected clock frequency before detecting all zero crossings of the signal. The resulting sampling vector is up sampled and applied to both data channels to obtain waveforms linearly spaced in frequency. In the spectra obtained by fast Fourier transforms, the impulse response elements are found at positions corresponding to fiber delays shown in Figure 1. A flat top windowing function is used to extract each element, From $H(\omega)$, both MDL and IL can be retrieved via singular value decomposition at every frequency. The resulting $\lambda(\omega)$ are the channel gains of the eigen modes of the device undertest [7,8].

Fiber device measurements

To calibrate the system, an elliptical core fiber is first measured. A fibre averaged spectrogram which is a combination of the spectral and temporal information in one image is composed. This allows a comprehensive visual representation of the DUT to be obtained.

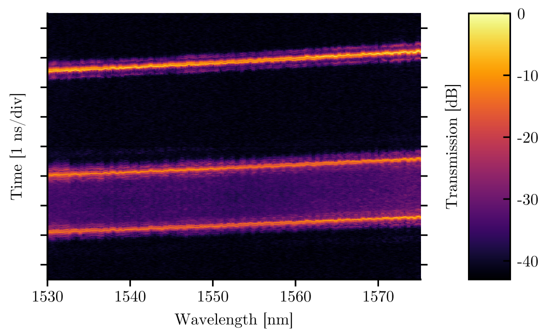

Figure 3: Spectrogram of an elliptical core fibre

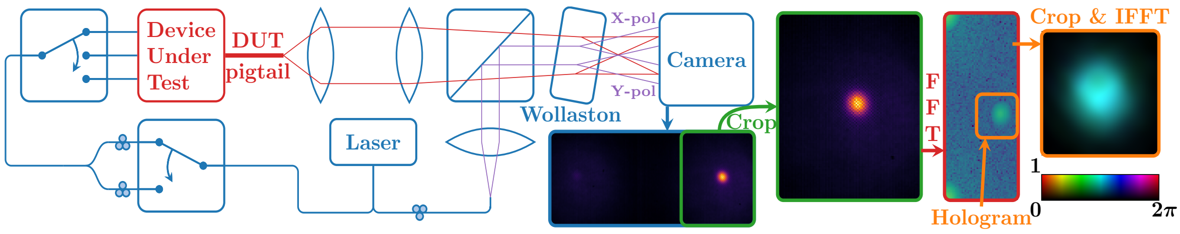

Figure 4: Setup diagram for a Digital Holography system including raw near infra-red camera and holograms

Off-axis Digital Holography analysis

Digital Holography provides an alternative characterisation tool for single device analysis [9, 10, 11]. In digital holography, the light emitting surface, in this case the facet of a fiber, is placed in a 4f optical setup as shown in Fig. 1. Note that the distances between the lenses in Fig. 4 are not drawn to scale to conserve space. The optical setup combines the light emitted from the facet, the signal, with a coherent flat-phase reference beam and images it magnified to the ratio of the lenses on the surface of the infrared camera. A Wollaston prism is used to spatially split both polarisations. The reference beam is placed under a slight angle, hence off-axis digital holography, which leads to fringes produced by the beating between the reference beam and the signal. Even though the camera only records the intensity of incident light and would thus destroy any phase information, it is still preserved in the fringe pattern and can therefore be extracted by subsequent digital signal processing (DSP).The DSP chain for digital holography starts with masking or cropping of a region of interest of the recorded camera frame as shown in the insets of Fig. 1. The Fourier transform is used to convert this region from the spatial domain, real-space, to the angular domain *k*-space. The intensity recorded by the camera can be described as

$$|s + r|^2 = |s|^2 + |r|^2 + sr^* + s^*r$$

Since signal and reference are placed under an angle, the beating terms appears at an angle as well, whereas the square terms are at DC. This allows for the extraction of the desired terms through masking or cropping. An inverse Fourier transform is used convert to real-space where now the full complex, i.e. both amplitude and phase, scaled image of the facet of the DUT is at our disposal. If the measurement apparatus is calibrated and aligned perfectly, this field can be used for subsequent processing.

The phase-corrected extracted fields are considered the result of the digital holography since the full polarisation-diverse complex field present at the facet of the DUT is known. However, these fields can be used for further processing and analysis, one particularly interesting use is the construction of a transfer matrix through digital demultiplexing. As shown in Figure 5, a suitable modal basis is chosen, and the overlap integral with the extracted field is calculated. Since this overlap is calculated digitally and the modal basis can be chosen freely, for example the mode profile of an optical fiber or device of interest, this technique is called digital demultiplexing. Figure 5: shows the extracted images for both polarisation obtained after FFT. From these images, transfer matrices can be constructed for detailed analysis.

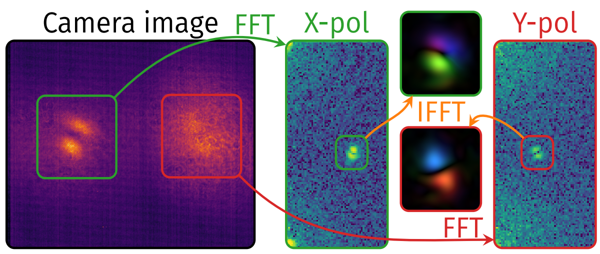

Figure 5: Signal processing: Fringe patterns are distributed spatially across the camera and are cropped and Fourier transformed to the angular domain, revealing the holograms. Inverse Fourier transformation of the hologram gives the extracted complex fields

Conclusions

In this paper, two fiber characterisation techniques are discussed. These techniques can be largely exploited for the emerging fibers such as few-mode multi-core, few-mode, multimode and hollow-core fiber analysis. Specific metrics such as mode dependent loss, insertion loss, group delay and differential group delay can be obtained from analysis of extracted transfer matrices.

Acknowledgements

We wish to thank Dr Simon Rommel for valuation discussions and technical contributions in constructing the OVNA.

References

[1] P. J. Winzer and D. T. Neilson, “From scaling disparities to integrated parallelism: A decathlon for a decade,” Journal of Lightwave Technology, vol. 35, no. 5, pp. 1099–1115, March 2017.

[2] D. Soma et al., “10.16 peta-bit/s dense sdm/wdm transmission over low-dmd 6-mode 19-core fibre across c+l band,” in 2017 European Conference on Optical Communication (ECOC), Sept 2017, pp. 1–3.

[3] J. J. A. van Weerdenburg et al., “Mode-multiplexed 16-qam transmission over 2400-km large-effective-area depressed-cladding 3-mode fiber,” in 2018 Optical Fiber Communications Conference and Exposition (OFC), March 2018, pp. 1–3.

[4] A. M. Velázquez-Benítezet al., “Scaling photonic lanterns for space-division multiplexing,” Sci. reports 8, 8897(2018).

[5] N. K. Fontaine et al., “Characterisation of space-division multiplexing systems using a swept-wavelength interferometer,” OFC (2013).

[6] S. Rommel et al., “Few-mode fiber, splice and SDM component characterisation by spatially-diverse optical vector network analysis,” Opt. Express25, 22347–22361 (2017).

[7] G. D. VanWiggeren and D. M. Baney, “Swept-wavelength interferometric analysis of multiport components,” IEEE Photonics Technology Letters, vol. 15, no. 9, pp. 1267–1269, Sept 2003.

[8] D. K. Gifford, B. J. Soller, M. S. Wolfe, and M. E. Froggatt, “Optical vector network analyser for single-scan measurements of loss, group delay, and polarisation mode dispersion,” Appl. Opt., vol. 44, no. 34, pp. 7282–7286, Dec. 2005

[9] M. Plöschner et al., “Seeing through chaos in multimode fibres,” Nat. Photonics9, 529 (2015).

[10] N. K. Fontaine et al., “Laguerre-gaussian mode sorter,” Nat. communications10, 1865 (2019).

[11] M. Mazuret al., “Characterisation of long multimode fiber links using digital holography,” OFC (2019).